The Company of
Biologists

RESEARCH ARTICLE

Residual force enhancement is reduced in permeabilized fiber bundles from *mdm* muscles

Dhruv Mishra and Kiisa C. Nishikawa*

ABSTRACT

Residual force enhancement (RFE) is the increase in steady-state force after active stretch relative to the force during isometric contraction at the same final length. The muscular dystrophy with myositis (*mdm*) mutation in mice, characterized by a small deletion in N2A titin, has been proposed to prevent N2A titin–actin interactions so that active *mdm* muscles are more compliant than wild type (WT). This decrease in active muscle stiffness is associated with reduced RFE. We investigated RFE in permeabilized soleus (SOL) and extensor digitorum longus (EDL) fiber bundles from WT and *mdm* mice. On each fiber bundle, we performed active and passive stretches from an average sarcomere length of 2.6–3.0 μm at a slow rate of 0.04 μm s^{-1}, as well as isometric contractions at the initial and final lengths. One-way ANOVA showed that SOL and EDL fiber bundles from *mdm* mice exhibited significantly lower RFE than WT mice ($P<0.0001$). This result is consistent with previous observations in single myofibrils and intact muscles. However, it contradicts the results from a previous study that appeared to show that compensatory mechanisms could restore titin force enhancement in single fibers from *mdm* psoas. We suggest that RFE measured previously in *mdm* single fibers was an artifact of the high variability in passive tension found in degenerating fibers, which begins after ~24 days of age. The results are consistent with the hypothesis that RFE is reduced in *mdm* skeletal muscles owing to impaired Ca^{2+}-dependent titin–actin interactions resulting from the small deletion in N2A titin.

KEY WORDS: Active stress after stretch, Extensor digitorum longus, Isometric stress, Passive stress after stretch, Soleus, Titin

INTRODUCTION

When skeletal muscles are stretched during activation, they exhibit a large increase in force (Abbott and Aubert, 1952; Flitney and Hirst, 1978; Katz, 1939), whereas consumption of energy decreases (Fenn, 1924; Ortega et al., 2015). When held at the stretched length, the force decreases and eventually reaches a steady state that is higher than the force produced during an isometric contraction at the same final length. The difference between steady-state force after active stretch and force during isometric contraction at the same final length is termed residual force enhancement (RFE; Edman et al., 1982). There is no widely accepted theory that provides a mechanism for RFE in skeletal muscles (Rassier and Herzog, 2004). Some alternative theories explain RFE based on contributions of

Department of Biological Sciences, Northern Arizona University, Flagstaff, AZ 86011, USA.

*Author for correspondence (Kiisa.Nishikawa@nau.edu)

D.M., 0000-0003-3652-6189; K.C.N., 0000-0001-8252-0285

cross-bridges and/or non-cross-bridge structures such as titin (Minozzo and de Lira, 2013).

Titin contributes up to 98% of passive force in myofibrils and sarcomeres (Bartoo et al., 1997; Granzier and Labeit, 2004). The titin protein has an I-band region that is composed of two spring-like elements, the proximal tandem Ig domains and the PEVK region (Gautel and Goulding, 1996). The N2A segment links the tandem Ig domains to the PEVK region (Linke et al., 1998). Earlier studies assumed that titin does not contribute to active muscle force production (e.g. Linke et al., 2002). However, numerous studies have suggested a significant role for titin in active muscle contraction (Horowits et al., 1986; Herzog, 2014; Leonard and Herzog, 2010; Linke, 2018; Monroy et al., 2012; Nishikawa et al., 2012). A role for titin in active muscle contraction was demonstrated in skeletal myofibers after exposure to low dose ionizing radiation (Horowits et al., 1986; Horowits and Podolsky, 1987), which showed that titin degradation reduced active force production and suggested that titin helps maintain active tension (Linke, 2018; Nishikawa et al., 2020).

More recently, several studies have demonstrated interactions between titin and calcium (Labeit et al., 2003; Tatsumi et al., 2001), as well as calcium-dependent interactions between titin and actin (Dutta et al., 2018; Kellermayer and Granzier, 1996), which have been suggested to play an important role in residual force enhancement (Leonard and Herzog, 2010; Tahir et al., 2020). Leonard and Herzog (2010) and Powers et al. (2014) demonstrated that titin force increases upon activation of skeletal muscles. They found that force increased faster with sarcomere length in active compared with passive myofibrils when stretched beyond overlap of the thick and thin filaments to eliminate production of force by cross-bridges. In contrast to wild-type (WT) muscles (Powers et al., 2014), Powers et al. (2016) observed that titin force fails to increase during active stretch of single muscular dystrophy with myositis (*mdm*) myofibrils stretched beyond overlap of thick and thin filaments. The *mdm* mutation (Lane, 1985) results in a small deletion in titin that includes 83 amino acids in the N2A region (Garvey et al. 2002). The observation by Powers et al. (2016) supports the idea that the *mdm* mutation reduces titin-based force in active muscles (Nishikawa et al., 2019, 2020) and supports the idea that the *mdm* mutation in mice is a good tool for assessing titin's role in active muscle.

Several recent studies have suggested that titin modulates RFE in skeletal muscles (Joumaa and Herzog, 2014; Shalabi et al., 2017; Tahir et al., 2020). In a study on skinned fibers from rabbit psoas muscles, Joumaa and Herzog (2014) found an increase in calcium sensitivity in the RFE state compared with purely isometric contraction. Furthermore, partial degradation of titin via trypsin treatment and subsequent osmotic compression of trypsin-treated fibers via dextran (T-500) eliminated the increase in calcium sensitivity (Joumaa and Herzog, 2014). These results suggest that titin regulates calcium sensitivity in RFE and that titin-based forces

can modify calcium sensitivity via a mechanism that is independent of myofilament lattice spacing. Another study demonstrated the presence of RFE in rabbit skeletal (psoas) but not in cardiac myofibrils (Shalabi et al., 2017), suggesting that the presence of RFE is related to differences in titin isoforms between skeletal (N2A) and cardiac muscles (N2B). Although consideration of RFE in cardiac muscle is beyond the scope of the present study, we note here that previous studies differ in reporting the presence (Boldt et al., 2020) or absence (Shalabi et al., 2017; Tomalka et al., 2019) of RFE in cardiac muscles. A recent study (Tahir et al., 2020) also showed that RFE was reduced in intact *mdm* soleus (SOL) muscles compared with WT.

In contrast to these previous studies that suggest a role for titin in RFE, Powers et al. (2017) reported similar average 'titin force enhancement' (TFE) in *mdm* and WT single psoas fibers. They defined TFE as the residual stress remaining in actively stretched individual fibers after subtracting the passive stress and contractile stress at a final sarcomere length of 3.2 μm (Powers et al., 2017). These results contradicted observations from a previous study in *mdm* myofibrils showing no increase in titin-based force upon activation (Powers et al., 2016), as well as a study on intact *mdm* SOL muscles (Tahir et al., 2020), which showed no RFE after subtracting passive stress after stretch from RFE.

The aim of our study was to revisit the question of whether RFE is reduced in fiber bundles from *mdm* SOL and extensor digitorum longus (EDL) muscles compared with WT. We included the relatively fast EDL and slow SOL muscles (Kushmerick et al., 1992) because previous observations suggested that the *mdm* mutation affects twitch and tetanic stress (Hessel et al., 2019) as well as eccentric work (Hessel and Nishikawa, 2017) to a greater extent in SOL than in EDL muscles, but RFE has not been quantified previously in *mdm* EDL muscles. We performed active stretch, passive stretch and isometric contraction from 2.6 to 3.0 μm on the same individual fiber bundles. We hypothesized that *mdm* fiber bundles from both SOL and EDL muscles will show reduced RFE compared with WT fibers, in contrast to the results of Powers et al. (2017). This result would be consistent with previous observations in single myofibrils (Powers et al., 2016) and intact muscles (Tahir et al., 2020). We also expected that RFE would be greater in the fast EDL than in the slower SOL on the basis of previous studies (Rassier, 2017; Tomalka et al., 2017).

MATERIALS AND METHODS
Heterozygous mice of the strain B6C3Fe a/a-Ttn *mdm*/J were obtained from the Jackson Laboratory (Bar Harbor, ME, USA) and a breeding colony was maintained to produce WT and homozygous recessive (*mdm*) mice. For experiments, WT mice (n=5) were 29–42 days of age (mean±s.e.m. age=35.8±2.7 days; mean body mass=19.5±1.8 g) and *mdm* mice were 16–30 days of age (mean age=25.0±2.5 days; mean body mass=4.1±0.7 g). Mice were housed in groups of 2–4 mice per cage, maintained on 12 h:12 h light:dark cycle at 22°C and were fed *ad libitum*. Mice of both sexes were killed via isoflurane overdose confirmed by cervical dislocation. For each mouse, 3–4 fiber bundles were harvested from the EDL and SOL (n=5 muscles per genotype), for a total of 16–20 fibers per muscle×genotype). We used fiber bundles from younger mice to reduce the possibility of fibrosis (Lopez et al., 2008) and degeneration (Heimann et al., 1996), which might affect the active and passive tension after stretch. EDL and SOL muscles were extracted from euthanized mice following standard procedures (Hakim and Nishikawa, 2013). The Institutional Animal Care and Use Committee at Northern Arizona University approved all husbandry and experimental protocols (nos. 18-002 and 21-001).
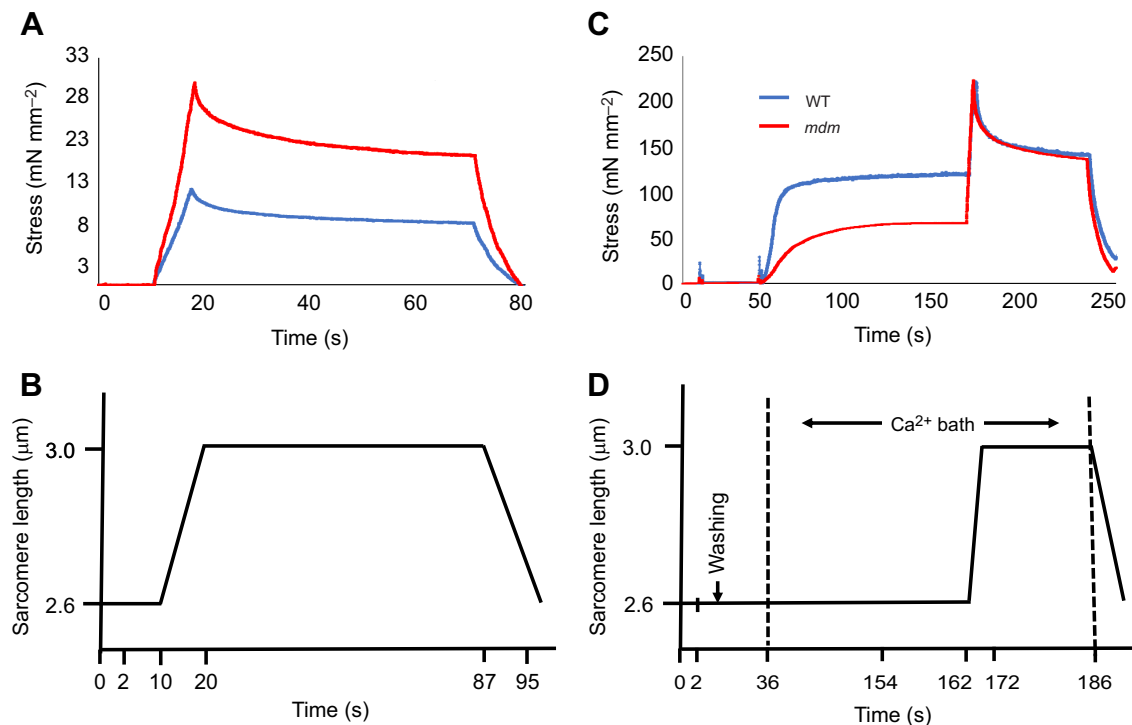
Preparation of skinned muscle fiber bundles
Fiber bundles were chosen for study because, like single fibers, sarcomere lengths can be imaged in real time during testing and force can be controlled by varying the calcium concentration, yet they are stronger and less likely to be damaged during isolation or active stretch. Skinned fiber bundles were prepared using standard techniques to minimize the contributions of endomysium to passive tension (Joumaa and Herzog, 2014). Extracted muscles were placed in a collection solution (in mmol l⁻¹: Tris 50, KCl 100, MgCl₂ 2, EGTA 1, pH 7.0) for 6 h at 4°C, then transferred to an overnight solution (in mmol l⁻¹: Tris 50, KCl 2, NaCl 100, MgCl₂ 2, EGTA 1, pH 7.0) with 1:1 glycerol for 12 h at 4°C, and finally placed in a long-term storage solution (collection solution with 1:1 glycerol) for 4–6 weeks at −20°C (Joumaa et al., 2007). To protect against protein degradation, protease inhibitor tablets (Complete®, Roche Diagnostics, Montreal, Quebec, Canada) were added to all solutions (1 tablet per 50 ml solution). Muscles were used 4–6 weeks after surgery. On the day of experiments, muscles were washed in relaxing solution (in mmol l⁻¹: potassium propionate 170, magnesium acetate 2.5, MOPS 20, K₂EGTA 5, ATP 2.5, pH 7.0) to remove the rigor–glycerol solution. Bundles of 4–5 fibers were then dissected from each muscle in a Petri dish filled with ice-cold relaxing solution and used immediately for experimentation. The solutions used during the experiments included relaxing solution, washing solution (in mmol l⁻¹: potassium propionate 185, magnesium acetate 2.5, MOPS 20, ATP 2.5, pH 7.0) and activating solution [in mmol l⁻¹: potassium propionate 170, magnesium acetate 2.5, MOPS 10, ATP 2.5, and CaEGTA and K₂EGTA mixed at different proportions to obtain a pCa (–log [Ca²⁺]) of 4.2, pH 7.0]. All experiments were conducted at room temperature (22°C). At this temperature, previous studies of rat and mouse SOL and EDL have found that these muscles retain ∼80–90% of their force at 35°C (James et al., 2015; Stephenson and Williams, 1985), although another study found a larger drop in the force of rat EDL and SOL at this temperature (Galler and Hilber, 1998).

Experimental apparatus
Using acetone and cellulose acetate (Merck, Darmstadt, Germany), each fiber bundle was glued lengthwise to a high-speed length controller on one end (Aurora Scientific, model 322C, Ontario, Canada) and a force transducer on the other end (Aurora Scientific, model 400A). Length control and force measurements were accomplished using an ASI802D data acquisition and control system (Aurora Scientific). The rig was connected to an inverted microscope (Leica, DMIRE2) with an ocular micrometer for measurement of fiber diameter (graticule 10 mm=100 divisions). The microscope was also fitted with a sarcomere length (SL) tracking camera (Aurora Scientific HVSL600A). Changes in SL were measured via SL tracking and acquisition software. The fiber rig was controlled using Linux software, which switches wells containing different solutions. In contrast to a previous study (Powers et al., 2017) in which laser diffraction was used to measure average SL, we used the SL tracking camera to measure initial and final SL. For measurement of SL, the Aurora 901B camera has a spatial resolution of 5 pixels μm⁻¹ at high magnification (50× optical lens of the inverted microscope) and 2 pixels μm⁻¹ at low magnification (20× optical lens of inverted microscope) at 300 frames s⁻¹ full frame (Aurora Scientific Inc., 2012).

Mechanical tests
The mechanical test protocols were designed to maximize RFE and minimize fiber damage by implementing a long stretch at a slow

Fig. 1. Stretch protocols. (A) Stress (mN mm^{-2}) and (B) sarcomere length (μm) of wild-type (WT; blue) and *mdm* (red) fiber bundles passively stretched from 2.6 to 3.0 μm. (C) Stress (mN mm^{-2}) and (D) sarcomere length (μm) of WT (blue) and *mdm* (red) fiber bundles actively stretched from 2.6 to 3.0 μm. Activation and relaxation are indicated by dashed lines in D.

velocity, as the magnitude of RFE increases with stretch amplitude but is largely independent of stretch rate (Abbott and Aubert, 1952; Herzog and Leonard, 2000; Sugi and Tsuchiya, 1988). To prevent slippage or breakage of fibers during the experiments, two pre-conditioning stretches in relaxing solution were performed before the start of each experiment. The pre-conditioning stretches from 2.6 to 3.0 μm were performed at a rate of 0.04 μm s^{-1}. After the pre-conditioning stretches, fiber bundles were passively stretched from 2.6 to 3.0 μm at 0.04 μm s^{-1} (Fig. 1), held isometrically for 60 s until steady-state force was attained, then moved to relaxing solution and returned to the original SL (2.6 μm). After a rest of 5 min, the fiber bundles were activated at 2.6 μm and were held isometrically for 118 s to reach steady-state force (Fig. 2). Thereafter, fiber bundles were actively stretched from 2.6 to 3.0 μm at 0.04 μm s^{-1} and held for 60 s, at which time the steady-state force at 3.0 μm was measured. Fiber bundles were then deactivated and returned to the starting SL. Finally, after a rest of 5 min, fiber bundles were passively stretched from 2.6 to 3.0 μm at a rate of 0.04 μm s^{-1}, then activated (139 s) to reach steady-state isometric stress at 3.0 μm (Fig. 2).
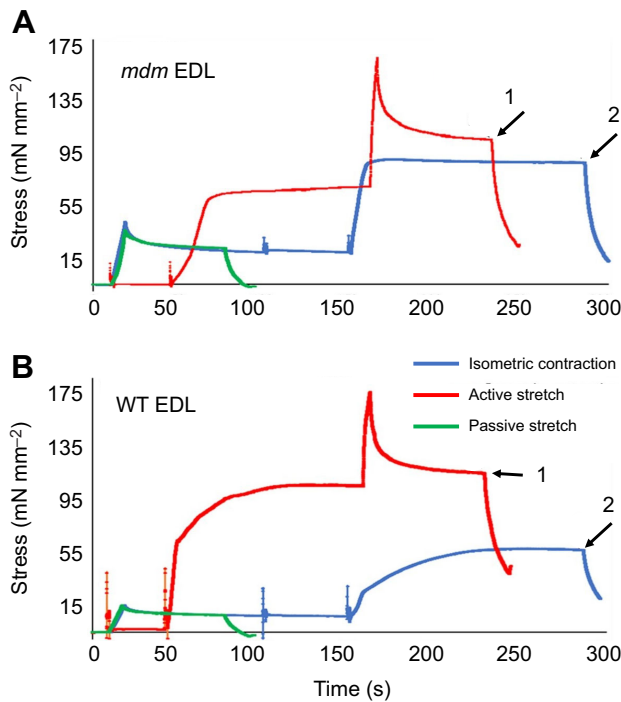
Stress (mN mm^{-2}) was calculated by dividing force by cross-sectional area, assuming a cylindrical shape of the fiber bundles (Powers et al., 2017). RFE was calculated by subtracting the steady-state force during isometric contraction at 3.0 μm from the steady-state force after active stretch to the same final SL (Fig. 2). We also calculated TFE as the stress after active stretch that remains after subtracting the total stress (passive+active) at the final SL of 3.0 μm (Powers et al., 2017). Finally, percentage of TFE (TFE%) as defined by Powers et al. (2017) was calculated as percentage of total stress following active stretch to final length (3.0 μm). Fibers in which no measurable force was observed after activation were eliminated from the trials. Based on this criterion, 5% of WT trials and 16% of *mdm* trials were removed from the final data set.

Data analysis

Statistical analysis was performed using JMP Pro14 and GraphPad Prism software. The Shapiro–Wilk test showed that the data were normally distributed ($P>0.05$). Levene's test showed that the variances differed significantly between genotypes ($P<0.05$). We corrected the data with non-homogeneous variances using Box–Cox transformation. To evaluate differences between WT and *mdm* fiber bundles, we used one-way ANOVA with genotype as the main effect. Because more than one fiber bundle from a single muscle was included in the data, we accounted for the within-muscle variation by including a random effect of muscle nested within genotype. Alpha values were set at 0.05 and the sample of 3–4 fiber bundles from $n=5$ mice per genotype was adequate to detect observed differences between means with power >0.8. The dependent variables were isometric stress at 2.6 μm, isometric stress at 3.0 μm, steady-state stress after passive stretch from 2.6 to 3.0 μm, steady-state stress after active stretch from 2.6 to 3.0 μm, RFE and TFE%. Data are presented as means±s.d. One-way ANOVA showed that the random effect of variation among muscles was significant for all dependent variables in both genotypes (WT and *mdm*). There were no significant correlations between mouse age and any dependent variables for either genotype (WT versus *mdm*) or muscle (EDL versus SOL; all $P>0.05$).
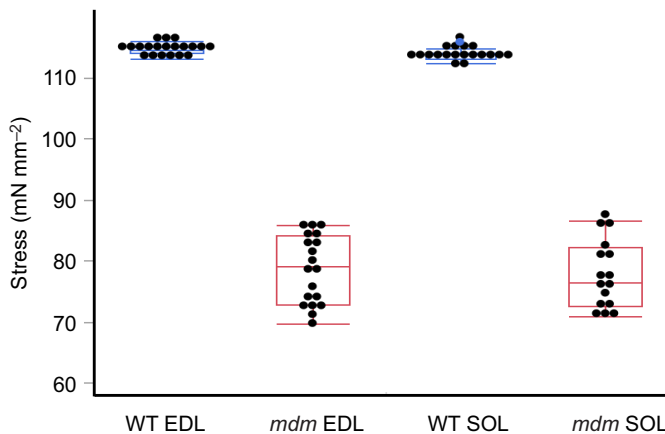
RESULTS

Total isometric stress at 2.6 μm (Fig. 3) was higher in WT EDL fiber bundles ($n=20$, mean±s.d.=114.5±0.27 mN mm^{-2}) than in *mdm* EDL fiber bundles ($n=19$, 78.5±5.77 mN mm^{-2}; ANOVA, $F=166.8$, $P<0.0001$). Similarly, total isometric stress was higher in WT SOL fiber bundles ($n=19$, 113.6±0.33 mm^2) at 2.6 μm (Fig. 3) compared with *mdm* SOL fiber bundles ($n=16$, 78.0±5.80 mN mm^{-2}; ANOVA, $F=166.18$, $P<0.0001$).
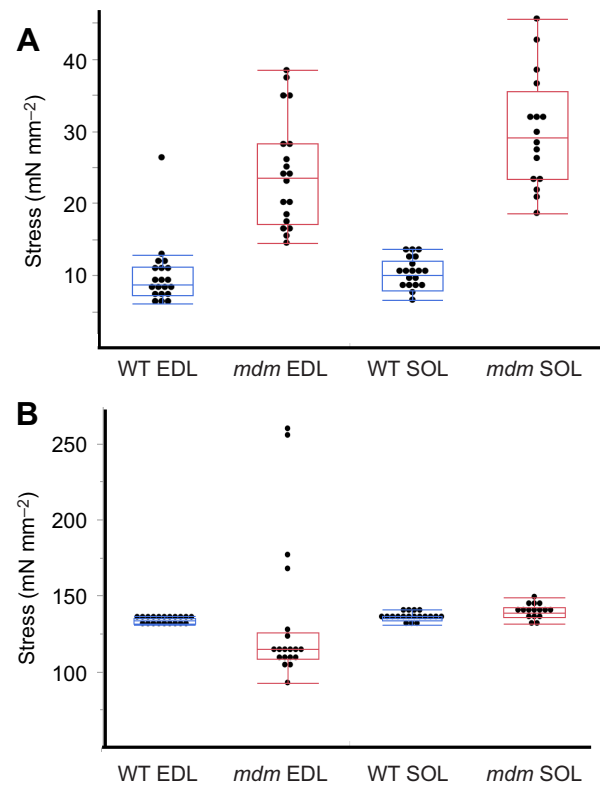
Fig. 2. Method for measuring residual force enhancement (RFE). RFE was calculated by subtracting the steady-state stress during isometric contraction (point 2) from the steady-state force after active stretch (point 1) at the final sarcomere length of 3.0 µm. (A) *Mdm* extensor digitorum longus (EDL) fiber bundle. (B) WT EDL fiber bundle.

Steady-state stress following passive stretch from 2.6 to 3.0 µm (Fig. 4A) was significantly higher in *mdm* EDL fiber bundles (n=19, 24.1±5.03 mN mm^{-2}) than in WT EDL fiber bundles (n=20, 9.8±2.82 mN mm^{-2}; ANOVA, F=35.0743, P<0.0004). Similarly, *mdm* SOL fiber bundles (n=16, 29.4±6.39 mN mm^{-2}) had higher passive stress following stretch from 2.6 to 3.0 µm than WT (n=19, 10.0±1.47 mN mm^{-2}; ANOVA, F=56.31, P<0.0001; Fig. 4A).

Fig. 3. Total isometric stress. Total isometric stress at 2.6 µm is reduced but more variable in *mdm* fiber bundles (red, n=5 muscles with 3–4 bundles per muscle, total 19 EDL and 16 *mdm* fiber bundles) from EDL (ANOVA, F=166.8, P<0.0001) and soleus (SOL) muscles (ANOVA, F=166.18, P<0.0001) compared with WT (blue, n=5 muscles with 3–4 bundles per muscle, total 20 EDL and 19 SOL fiber bundles). Boxes indicate 25% and 75% quartiles, mean and standard deviation.
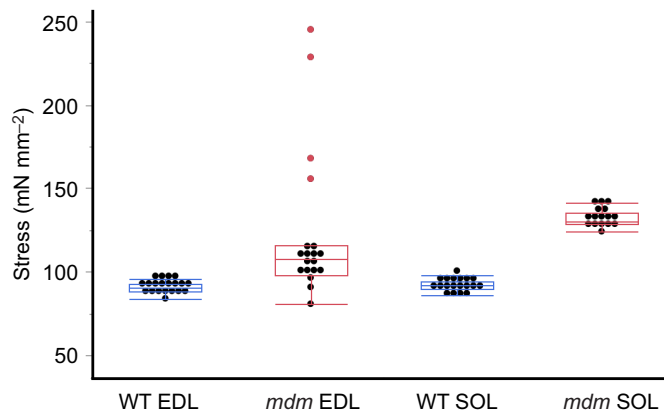
Fig. 4. Steady-state stress after passive and active stretch. (A) Steady-state stress (mN mm^{-2}) after passive stretch was larger and more variable in *mdm* fiber bundles (red, n=5 muscles with 3–4 bundles per muscle, total 19 EDL and 16 *mdm* fiber bundles) compared with WT (blue, n=5 muscles with 3–4 bundles per muscle, total 20 EDL and 19 SOL fiber bundles) in both EDL (ANOVA, F=35.07, P<0.0004) and SOL muscles (ANOVA, F=56.31, P<0.0001). (B) Stress after active stretch was higher in *mdm* (red) than WT (blue) SOL fiber bundles (ANOVA, F=12.786, P<0.0072). However, stress after active stretch was similar between *mdm* (red) and WT (blue) EDL fiber bundles. Boxes indicate 25% and 75% quartiles, mean and standard deviation. For WT EDL, the upper and lower quartiles are too close to the mean to be seen at this resolution.

Steady-state stress after active stretch (Fig. 4B) was not significantly different between *mdm* EDL fiber bundles (132.5±16.70 mN mm^{-2}) and WT EDL fiber bundles (133.4±0.94 mN mm^{-2}, ANOVA, F=2.0159, P=0.1934). However, *mdm* SOL fiber bundles (Fig. 4B) had a significantly higher active stress after stretch (139.4±1.61 mN mm^{-2}) than WT fiber bundles (135.6±1.76 mN mm^{-2}; ANOVA, F=12.786, P=0.0072).

Total isometric stress at 3.0 µm (Fig. 5) was significantly higher in *mdm* EDL (122.1±15.21 mN mm^{-2}) compared with WT EDL (90.4±0.88 mN mm^{-2}; ANOVA, F=49.09, P<0.0001). Similarly, *mdm* SOL (131.7±2.15 mN mm^{-2}) had significantly higher total isometric stress at 3.0 µm than WT SOL fiber bundles (91.6±2.83 mN mm^{-2}; ANOVA, F=605.09, P<0.0001).

Significantly lower RFE was observed in *mdm* EDL (10.4±3.60 mN mm^{-2}) and SOL (7.7±1.05 mN mm^{-2}) fiber bundles compared with WT EDL (43.0±1.75 mN mm^{-2}; ANOVA, F=199.36, P<0.0001) and SOL fiber bundles (43.9±1.44 mN mm^{-2}; ANOVA, F=1815.34, P<0.0001), respectively (Fig. 6). *Mdm* fiber bundles from both EDL (−10±2.96%; Fig. 7A) and SOL (−16±4.7%; Fig. 7B) showed no TFE%. After subtracting the passive stress component from RFE, TFE% was significantly lower in *mdm* fiber bundles compared with WT EDL (26±2.14%; ANOVA, F=316.9, P<0.0001). Similarly, TFE% was lower in *mdm*
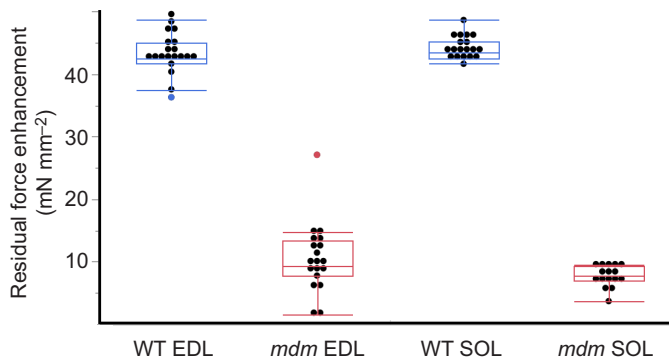
Fig. 5. Total steady-state isometric stress. Total steady-state isometric stress at 3.0 µm was higher and more variable in *mdm* fiber bundles (red, *n*=5 muscles with 3–4 bundles per muscle, total 19 EDL and 16 *mdm* fiber bundles) from EDL (ANOVA, *F*=49.09, *P*<0.0001) and SOL (ANOVA, *F*=605.09, *P*<0.0001) muscles compared with WT (blue, *n*=5 muscles with 3–4 bundles per muscle, total 20 EDL and 19 SOL fiber bundles). Boxes indicate 25% and 75% quartiles, mean and standard deviation. For *mdm* EDL, the upper quartile and the standard deviation cannot be distinguished at this resolution.

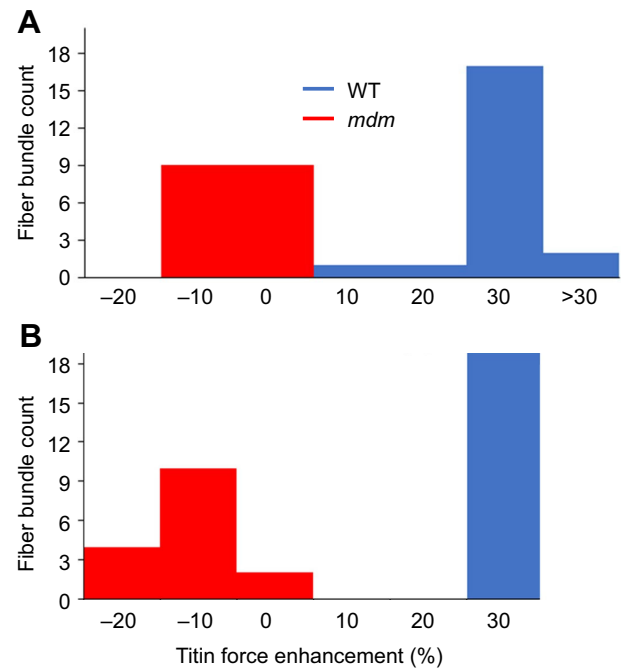SOL fiber bundles compared with WT SOL fiber bundles (25±0.89%; ANOVA, *F*=219.6, *P*<0.0001).

DISCUSSION

In summary, we found that total isometric stress was higher and less variable in WT EDL and SOL fiber bundles than in *mdm* fiber bundles at an SL of at 2.6 µm but was higher and more variable in *mdm* fiber bundles than WT at 3.0 µm in both muscles. Stress following passive stretch from 2.6 to 3.0 µm was also higher and more variable in *mdm* fiber bundles than WT in both muscles, whereas total stress following active stretch was significantly higher in *mdm* SOL but not in *mdm* EDL. RFE was significantly lower in *mdm* fiber bundles than WT in both muscles, and no fibers of any muscles exhibited positive values of TFE%.

Reduced total isometric stress in *mdm* skeletal muscles compared with WT at shorter SLs near the plateau of the length–tension relationship (see Fig. 3) has also been found in previous studies (Huebsch et al., 2005; Monroy et al., 2012; Powers et al., 2016, 2017; Tahir et al., 2020). This reduction in contractile stress in *mdm* is likely due at least in part to impaired transmission of cross-bridge

Fig. 6. Residual force enhancement. RFE was reduced in *mdm* (red, *n*=5 muscles with 3–4 bundles per muscle, total 19 EDL and 16 *mdm* fiber bundles) fiber bundles from EDL (*F*=199.36; *P*<0.0001) and SOL (*F*=1815.34; *P*<0.0001) compared with WT (blue, *n*=5 muscles with 3–4 bundles per muscle, total 20 EDL and 19 SOL fiber bundles). Boxes indicate 25% and 75% quartiles, mean and standard deviation.

Fig. 7. Fiber bundle count for titin force enhancement (TFE; %). (A) EDL fiber bundles (*mdm* *n*=19 and WT *n*=20) and (B) SOL fibers (WT *n*=19 and *mdm* *n*=16). *Mdm* (red) show reduced TFE% in both EDL (−10±2.96%) and SOL (−16%±4.7) fiber bundles as compared with WT (blue) EDL (26±2.14%; *F*=316.9, *P*<0.0001) and SOL (25±0.89%; *F*=219.6, *P*<0.0001) fiber bundles, which show >10% TFE.

force from the A-band to the Z-line (Horowits et al., 1986). In the present study, the total isometric stress was higher in *mdm* skeletal muscles compared with WT at the longer SL (3.0 µm), presumably owing to higher passive tension (see below). Values of total isometric stress at comparable lengths have not been reported in previous studies, but Powers et al. (2017) found no difference between *mdm* and WT fibers at an SL of 5.2 µm.

Steady-state stress following passive stretch was significantly reduced in WT EDL and SOL fiber bundles compared with fiber bundles from *mdm* mice (see Fig. 4A,B). Earlier studies also found higher and more variable passive stress in *mdm* fibers (Powers et al., 2017) and intact muscles (Tahir et al., 2020) compared with WT. Higher passive stress could be due to alterations in exon splicing in the PEVK region of titin that could potentially lead to expression of shorter and stiffer titin isoforms in *mdm* muscles (Hettige, 2021). In addition, high collagen content in *mdm* muscles has also been demonstrated (via colorimetric hydroxyproline assay) as a potential contributor to higher passive stress (Powers et al., 2017). Higher passive stress accounts for the higher total contractile stress at 3.0 µm (sum of active stress plus steady-state passive stress) in *mdm* muscles, which was found in the present study and has also been found in previous studies (Powers et al., 2017; Tahir et al., 2020; Hessel et al., 2019).

Steady-state stress was larger after active stretch than after passive stretch in WT and *mdm* EDL and SOL fiber bundles (Fig. 4A,B). We found that steady-state stress after active stretch was larger in *mdm* SOL than in WT SOL (Fig. 4B). In contrast, Powers et al. (2017) found no difference between passive and active stress after stretch to very long SLs (5.2 µm) in psoas fibers from *mdm* mice, likely owing to much higher passive tension at the longer sarcomere length. They also found no difference in active stress after stretch between *mdm* and WT fibers.

RFE, the increase in steady-state stress after active stretch (Abbott and Aubert, 1952; Edman et al., 1982), is a long-known property of skeletal muscles. Our results showed reduced RFE in *mdm* fiber bundles from both SOL and EDL compared with WT (see Fig. 6). The small amount of RFE that remains in *mdm* fiber bundles could be due to the presence of glutamine-rich motifs in the PEVK region of titin, which have a high affinity for Ca^{2+} (Labeit et al., 2003). This result is consistent with previous observations from *mdm* myofibrils (Powers et al., 2016) and intact muscles (Tahir et al., 2020).

Similar to Hessel et al. (2017), we found that RFE was higher in EDL than in SOL. This may be due to expression of a larger titin isoform in SOL than EDL (Freiburg et al., 2000; Prado et al., 2005; Buck et al., 2014). Prado et al. (2005) demonstrated that passive tension is higher in muscles with shorter titin isoforms (i.e. EDL) compared with muscles with longer titin isoforms (e.g. SOL; see Hettige, 2021 for isoform expression in *mdm* muscles). Cornachione et al. (2016) also demonstrated that increasing size of titin isoforms was related to decreasing passive tension in rabbit SOL, psoas and ventricular myofibrils. Although they did not quantify RFE directly, they found that the difference in force between passive and active ramp stretches of the same myofibril also decreased with the size of the titin isoform in these muscles.

Powers et al. (2017) reported the presence of TFE in nine of 11 *mdm* fibers whereas TFE was absent in only two *mdm* fibers. In the present study, we found no TFE in any *mdm* fiber bundles from either SOL or EDL muscles (see Fig. 7). Several factors may account for the difference in results between the present study and those of Powers et al. (2017). Most importantly, we used *mdm* fiber bundles from young mice (16–30 days old) compared with the older (27–41 days old) *mdm* muscles used by Powers et al. (2017). Muscle degeneration starts as early as 1–2 weeks of age in SOL but not until 3–4 weeks of age in tibialis anterior (Heimann et al., 1996). Several studies have found that *mdm* skeletal muscles have normal sarcomere structure at ∼24–29 days of age (Hessel et al., 2019; Lopez et al., 2008; Witt et al., 2004).

Powers et al. (2017) found significant structural changes in the *mdm* psoas muscles they studied, including small fiber diameter, large numbers of central nuclei, and fibrosis (see their Figs 3 and 4). They were only able to measure SL using laser diffraction in less than 20% of their fibers, whereas Hessel et al. (2019) were able to measure SL using laser diffraction in all of their 24- to 29-day-old EDL fibers. In the present study, sarcomere structure appeared normal and SL could be quantified from video images in all of the fiber bundles tested. Based on the older age of the *mdm* muscles used in Powers et al.'s (2017) study, it appears likely that sarcomere degeneration and fibrosis led to high variability in tension after both passive and active stretching, and ultimately to the observation of TFE in a large number of *mdm* fibers. However, in the present study, RFE was reduced significantly and we failed to observe TFE in any *mdm* fiber bundles from EDL or SOL at 16–30 days of age.

Recent studies have proposed a role for titin in RFE (Leonard and Herzog, 2010; Nishikawa et al., 2012; Rode et al., 2009; Shalabi et al., 2017). Both Leonard and Herzog (2010) and Powers et al. (2014) showed that Ca^{2+}-activated myofibrils stretched beyond overlap of thick and thin filaments have a higher titin-based force than passively stretched myofibrils at the same average sarcomere length; they found a steeper increase in force in active WT myofibrils than in passive WT myofibrils when stretched to very long sarcomere lengths beyond overlap of the thick and thin filaments. In contrast, Powers et al., (2016) found no difference in slope between actively and passively stretched *mdm* myofibrils, which suggests that titin force fails to increase upon activation in *mdm* myofibrils due to the small deletion in the N2A region of titin.

Leonard and Herzog (2010) and Powers et al. (2014, 2016) suggested binding of titin to actin as a mechanism for increasing titin force in active muscle. Nishikawa et al. (2012, Nishikawa, 2016) proposed that if N2A titin binds to actin in active muscle, then tandem Ig domains of titin would straighten at low force when skeletal muscles are passively stretched. When stretched actively, only the PEVK region of titin would extend at high force. In recent experiments, Dutta et al. (2018) demonstrated that N2A titin binds to actin and thin filaments, and that Ca^{2+} increases the strength and stability of N2A titin–actin interactions (Adewale and Ahn, 2021; Tsiros et al., 2021), supporting the hypothesis that titin plays a regulatory role in active muscle contraction. It has also been proposed that the *mdm* mutation prevents N2A titin–actin interactions, so that active *mdm* muscles are more compliant than WT muscles (Monroy et al., 2017; Dutta et al., 2018; Nishikawa et al., 2020). The decrease in active muscle stiffness should be associated with a reduction in RFE in *mdm* muscles (Powers et al., 2014, 2016; Tahir et al., 2020).

Conclusions

The findings of the present study that RFE was reduced and TFE was absent in 16- to 30-day-old EDL and SOL muscles from *mdm* mice are consistent with previous data from single myofibrils demonstrating that titin force increases upon calcium activation in WT myofibrils stretched beyond overlap for the thick and thin filaments (Powers et al., 2014), but not in *mdm* myofibrils under the same conditions (Powers et al., 2016). They are also consistent with observations that RFE is reduced in intact *mdm* SOL muscles (Tahir et al., 2020). The conflicting observations from an earlier study (Powers et al., 2017), which appeared to show that compensatory mechanisms could restore TFE in single fibers from *mdm* psoas, are likely explained by degeneration and fibrosis. The present study is also consistent with the idea that the *mdm* mutation affects N2A titin–actin interactions (Dutta et al., 2018), which reduces titin-based force in active muscles (Powers et al., 2016; Monroy et al., 2017), thereby decreasing RFE and TFE.

References
Abbott, B. C. and Aubert, X. M. (1952). The force exerted by active striated muscle during and after change of length. *J. Physiol.* **117**, 77-86. doi:10.1113/jphysiol.1952.sp004755
Adewale, A. O. and Ahn, Y.-H. (2021). Titin N2A domain and its interactions at the sarcomere. *Int. J. Mol. Sci.* **22**, 7563. doi:10.3390/ijms22147563

Aurora Scientific Inc (2012). 900A/901A/901B VSL/HVSL Instruction manual. Program (V3.000). http://bulletins.aurorascientific.com/manuals/900B_901A_901B.v3.000.Manual.pdf, 21-30.

Bartoo, M. L., Linke, W. A. and Pollack, G. H. (1997). Basis of passive tension and stiffness in isolated rabbit myofibrils. *Am. J. Physiol.* **273**, C266-C276. doi:10.1152/ajpcell.1997.273.1.C266

Boldt, K., Han, S.-W., Joumaa, V. and Herzog, W. (2020). Residual and passive force enhancement in skinned cardiac fibre bundles. *J. Biomech.* **109**, 109953. doi:10.1016/j.jbiomech.2020.109953

Buck, D., Smith, J. E., Chung, C. S., Ono, Y., Sorimachi, H., Labeit, S. and Granzier, H. L. (2014). Removal of immunoglobulin-like domains from titin's spring segment alters titin splicing in mouse skeletal muscle and causes myopathy. *J. Gen. Physiol.* **143**, 215-230. doi:10.1085/jgp.201311129

Cornachione, A. S., Leite, F., Bagni, M. A. and Rassier, D. E. (2016). The increase in non-crossbridge forces after stretch of activated striated muscle is related to titin isoforms. *Am. J. Physiol. Cell Physiol.* **310**, C19-C26. doi:10.1152/ajpcell.00156.2015

Dutta, S., Tsiros, C., Sundar, S. L., Athar, H., Moore, J., Nelson, B., Gage, M. J. and Nishikawa, K. (2018). Calcium increases titin N2A binding to F-actin and regulated thin filaments. *Sci. Rep.* **8**, 1-11. doi:10.1038/s41598-018-32952-8

Edman, K. A. P., Elzinga, G. and Noble, M. I. (1982). Residual force enhancement after stretch of contracting frog single muscle fibers. *J Gen. Physiol.* **80**, 769-784. doi:10.1085/jgp.80.5.769

Fenn, W. O. (1924). The relation between the work performed and the energy liberated in muscular contraction. *J. Physiol.* **58**, 373-395. doi:10.1113/jphysiol.1924.sp002141

Flitney, F. W. and Hirst, D. G. (1978). Cross-bridge detachment and sarcomere "give" during stretch of active frog's muscle. *J. Physiol.* **276**, 449-465. doi:10.1113/jphysiol.1978.sp012246

Freiburg, A., Trombitas, K., Hell, W., Cazorla, O., Fougerousse, F., Centner, T., Kolmerer, B., Witt, C., Beckmann, J., Gregorio, C. et al. (2000). Series of exon-skipping events in titin's elasticspring region as the structural basis for myofibrillar elastic diversity. *Circ. Res.* **86**, 1114-1121. doi:10.1161/01.RES.86.11.1114

Galler, S., Hilber, K. (1998). Tension/stiffness ratio of skinned rat skeletal msucle fibre types at various temperatures. *Acta Physiol. Scand.* **162**, 119-126. doi:10.1046/j.1365-201X.1998.0272f.x

Garvey, S. M., Rajan, C., Lerner, A. P., Frankel, W. N. and Cox, G. A. (2002). The muscular dystrophy with myositis (*mdm*) mouse mutation disrupts a skeletal muscle-specific domain of titin. *Genomics* **79**, 146-149. doi:10.1006/geno.2002.6685

Gautel, M. and Goulding, D. (1996). A molecular map of titin/connectin elasticity reveals two different mechanisms acting in series. *FEBS Lett.* **385**, 11-14. doi:10.1016/0014-5793(96)00338-9

Granzier, H. L. and Labeit, S. (2004). The giant protein titin: a major player in myocardial mechanics, signaling and disease. *Circ. Res.* **94**, 284-295. doi:10.1161/01.RES.0000117769.88862.F8

Hakim, C. H., Wasala, N. B. and Duan, D. (2013). Evaluation of muscle function of the extensor digitorum longus muscle *ex vivo* and tibialis anterior muscle *in situ* in mice. *J. Vis. Exp.* **72**, e50183.

Heimann, P., Menke, A., Rothkegel, B. and Jockusch, H. (1996). Overshooting production of satellite cells in murine skeletal muscle affected by the mutation "muscular dystrophy with myositis" (mdm chr2). *Cell Tissue Res.* **283**, 435-441. doi:10.1007/s004410050554

Herzog, W. (2014) The role of titin in eccentric muscle contraction. *J. Exp. Biol.* **217**, 2825-2833.

Herzog, W. and Leonard, T. L. (2000). The history dependence of force production in mammalian skeletal muscle following stretch-shortening and shortening–stretch cycles. *J. Biomech.* **33**, 531-542. doi:10.1016/S0021-9290(99)00221-3

Hessel, A. L. and Nishikawa, K. C. (2017). Effects of a titin mutation on negative work during stretch-shortening cycles in skeletal muscles. *J. Exp. Biol.* **220**, 4177-4185. doi:10.1242/jeb.163204

Hessel, A. L., Joumaa, V., Eck, S., Herzog, W. and Nishikawa, K. C. (2019). Optimal length, calcium sensitivity and twitch characteristics of skeletal muscles from *mdm* mice with a deletion in N2A titin. *J. Exp. Biol.* **222**, jeb200840. doi:10.1242/jeb.200840

Hettige, P. (2021). Comparative transcriptomic analysis of extensor digitorum longus (EDL), psoas and soleus (SOL) muscles from muscular dystrophy with myositis (*mdm*) mice. PhD dissertation, University of Massachusetts Lowell.

Horowits, R. and Podolsky, R. J. (1987). The positional stability of thick filaments in activated skeletal muscle depends on sarcomere length: evidence for the role of titin filaments. *J. Cell. Biol.* **105**, 1540-8140.

Horowits, R., Kempner, E. S., Bisher, M. E. and Podolsky, R. J. (1986). A physiological role of titin and nebulin in skeletal muscle. *Nature* **323**, 160-164.

Huebsch, K. A., Kudryashova, E., Wooley, C. M., Sher, R. B., Seburn, K. L., Spencer, M. J. and Cox, G. A. (2005). *Mdm* muscular dystrophy: interactions with calpain 3 and a novel functional role for titin's N2A domain. *Hum. Mol. Genet.* **14**, 2801-2811. doi:10.1093/hmg/ddi313

James, R. S., Tallis, J. and Angilletta, M. J. (2015). Regional thermal specialisation in a mammal: temperature affects power output of core muscle

more than that of peripheral muscle in adult mice (*Mus musculus*). *J. Comp. Physiol. B* **185**, 135-142. doi:10.1007/s00360-014-0872-6

Joumaa, V. and Herzog, W. (2014). Calcium sensitivity of residual force enhancement in rabbit skinned fibers. *Am. J. Physiol. Cell Physiol.* **307**, 395-401. doi:10.1152/ajpcell.00052.2014

Joumaa, V., Rassier, D. E. and Leonard, T. R. (2007). Passive force enhancement in single myofibrils. *Pflugers Arch Eur J Physiol.* **455**, 367-371. doi:10.1007/s00424-007-0287-2

Katz, B. (1939). The relation between force and speed in muscular contraction. *J. Physiol.* **96**, 45-64. doi:10.1113/jphysiol.1939.sp003756

Kellermayer, M. S. Z. and Granzier, H. L. (1996). Calcium-dependent inhibition of in vitro thin-filament motility by native titin. *FEBS Lett.* **380**, 281-286. doi:10.1016/0014-5793(96)00055-5

Kushmerick, M. J., Moerland, T. S. and Wiseman, R. W. (1992). Mammalian skeletal muscle fibers distinguished by contents of phosphocreatine, ATP, and Pi. *Proc. Natl. Acad. Sci. USA* **89**, 7521-7525. doi:10.1073/pnas.89.16.7521

Labeit, D., Watanabe, K., Witt, C., Fujita, H., Wu, Y., Lahmers, S., Funck, T., Labeit, S. and Granzier, H. L. (2003). Calcium-dependent molecular spring elements in the giant protein titin. *Proc. Natl. Acad. Sci. USA.* **100**, 13716-13721. doi:10.1073/pnas.2235652100

Lane, P. W. (1985). Muscular dystrophy with myositis (*mdm*). *Mouse News Lett.* **73**, 18.

Leonard, T. R. and Herzog, W. (2010). Regulation of muscle force in the absence of actin-myosin based cross bridge interaction. *Am J Physiol. Cell Physiol.* **299**, C14-C20. doi:10.1152/ajpcell.00049.2010

Linke, W. A. (2018). Titin gene and protein and functions in passive and active muscle. *Annu. Rev. Physiol.* **80**, 389-411. doi:10.1146/annurev-physiol-021317-121234

Linke, W. A., Ivemeyer, M., Mundel, P., Stockmeier, M. R. and Kolmerer, B. (1998). Nature of PEVK-titin elasticity in skeletal muscle. *Proc. Natl. Acad. Sci. USA* **95**, 8052-8057.

Linke, W. A., Kulke, M., Li, H., Fujita-Becker, S., Neagoe, C., Manstein, D. J., Gautel, M. and Fernandez, M. J. (2002). PEVK domain of titin: an entropic spring with actin binding properties. *J. Struct. Biol.* **137**, 197-205. doi:10.1006/jsbi.2002.4468

Lopez, M. A., Pardo, P. S., Cox, G. A. and Boriek, A. M. (2008). Early mechanical dysfunction of the diaphragm in the muscular dystrophy with myositis (*mdm*) model. *Am. J. Physiol. Cell Physiol.* **295**, C1092-C1102. doi:10.1152/ajpcell.16.2008

Monroy, J. A., Powers, K. L., Gilmore, L. A., Uyeno, T. A., Lindstedt, S. L. and Nishikawa, K. C. (2012). What is the role of titin in active muscle? *Exerc. Sport Sci. Rev.* **40**, 73-78. doi:10.1097/JES.0b013e31824580c6

Minozzo, F. C. and de Lira, C. A. B. (2013). Muscle residual force enhancement: a brief review. *Clinics (Sao Paulo)* **68**, 269-274. doi:10.6061/clinics/2013(02)R01

Monroy, J. A., Powers, K. L., Pace, C. M., Uyeno, T. and Nishikawa, K. C. (2017). Effects of activation on the elastic properties of intact soleus muscles with a deletion in titin. *J. Exp. Biol.* **220**, 828-836. doi:10.1242/jeb.139717

Nishikawa, K. (2016). Eccentric contraction: unraveling mechanisms of force enhancement and energy conservation. *J. Exp. Biol.* **219**, 189-196. doi:10.1242/jeb.124057

Nishikawa, K. C., Monroy, J. A., Uyeno, T. E., Yeo, S. H., Pai, D. K. and Lindstedt, S. L. (2012). Is titin a 'winding filament'? A new twist on muscle contraction. *Proc. R Soc. B. Biol.* **279**, 981-990.

Nishikawa, K., Dutta, S., DuVall, M., Nelson, B., Gage, M. J. and Monroy, J. A. (2019). Ca^{2+}-dependent titin–thin filament interactions in muscle: observations and theory. *J. Muscle Res. Cell Motil.* **41**, 125-139. doi:10.1007/s10974-019-09540-y

Nishikawa, K., Lindstedt, S., Hessel, A. L. and Mishra, D. (2020). N2A titin: signaling hub and mechanical switch skeletal muscle. *Int. J. Mol. Sci.* **21**, 3974. doi:10.3390/ijms21113974

Nishikawa, K., Mishra, D. and Nishikawa, K. C. (2022). Residual force enhancement is reduced in permeabilized fiber bundles from *mdm* muscles. Dryad, Dataset, doi:10.5061/dryad.m37pvmd47

Ortega, J. O., Lindstedt, S. L., Nelson, F. E., Jubrias, S. A., Kushmerick, M. J. and Conley, K. E. (2015). Muscle force, work and cost: a novel technique to revisit the Fenn effect. *J. Exp. Biol.* **218**, 2075-2082.

Powers, K., Schappacher-Tilp, G., Jinha, A., Leonard, T., Nishikawa, K. and Herzog, W. (2014). Titin force is enhanced in actively stretched skeletal muscles. *J. Exp. Biol.* **217**, 3629-3696.

Powers, K., Nishikawa, K., Joumaa, V. and Herzog, W. (2016). Decreased force enhancement in skeletal muscle sarcomeres with a deletion in titin. *J. Exp. Biol.* **219**, 1311-1316.

Powers, K., Joumaa, V., Jinha, A., Moo, E. K., Smith, I. C., Nishikawa, K. and Herzog, W. (2017). Titin force enhancement following active stretch of skinned skeletal muscle fibres. *J. Exp. Biol.* **220**, 3110-3118.

Prado, G. L., Makarenko, I., Andresen, C., Krüger, M., Opitz, C. A. and Linke, W. A. (2005). Isoform diversity of giant proteins in relation to passive and active contractile properties of rabbit skeletal muscles. *J. Gen. Physiol.* **126**, 461-480.

Rassier, D. E. (2017). Sarcomere mechanics in striated muscles: from molecules to sarcomeres to cells. *Am. J. Physiol. Cell Physiol.* **313**, C134-C145.

Rassier, D. E. and Herzog, W. (2004). Considerations on the history dependence of muscle contraction. *J. Appl. Physiol.* **96**, 419-427. doi:10.1152/japplphysiol.00653.2003

Rode, C., Siebert, T. and Blickhan, R. (2009). Titin-induced force enhancement and force depression: A "sticky spring" mechanism in muscle contractions? *J. Theor. Biol.* **259**, 350-360. doi:10.1016/j.jtbi.2009.03.015

Shalabi, N., Cornachione, A., De Siouza Leite, F., Vengallatorre, S. and Rassier, D. E. (2017). Residual force enhancement is regulated by titin in skeletal and cardiac myofibrils. *J. Physiol.* **595**, 2085-2098. doi:10.1113/JP272983.

Stephenson, D. G. and Williams, D. A. (1985). Temperature-dependent calcium sensitivity changes in skinned muscle fibres of rat and toad. *J. Physiol.* **360**, 1-12. doi:10.1113/jphysiol.1985.sp015600

Sugi, H. and Tsuchiya, T. (1988). Stiffness changes during enhancement and deficit of isometric force by slow length changes in frog skeletal muscle fibres. *J. Physiol.* **407**, 215-229. doi:10.1113/jphysiol.1988.sp017411

Tahir, U., Monroy, J. A., Rice, N. A. and Nishikawa, K. C. (2020). Effects of a titin mutation on force enhancement and force depression in mouse soleus muscles. *J. Exp. Biol.* **223**, jeb197038. doi:10.1242/jeb.197038

Tatsumi, R., Maeda, K., Hattori, A. and Takahashi, K. (2001). Calcium binding to an elastic portion of connectin/titin filaments. *J. Muscle Res. Cell Motil.* **22**, 149-162. doi:10.1023/A:1010349416723

Tomalka, A., Rode, C., Schumacher, J. and Siebert, T. (2017). The active force–length relationship is invisible duringextensive eccentric contractions in skinned skeletal muscle fibres. *Proc. R. Soc. B* **284**, 20162497. doi:10.1098/rspb.2016.2497

Tomalka, A., Röhrle, O., Han, J.-C., Pham, T., Taberner, A. J. and Siebert, T. (2019). Extensive eccentric contractions in intact cardiac trabeculae: revealing compelling differences in contractile behaviour compared to skeletal muscles. *Proc. R. Soc. B* **286**, 20190719. doi:10.1098/rspb.2019.0719

Tsiros, C., Punch, E., Schaffter, E., Apel, S. and Gage, M. J. (2021). Identification of the domains within the N2A region of titin that regulate binding to actin. *Biochem. Biophys. Res. Commun.* **589**, 147-151. doi:10.1016/j.bbrc.2021.12.025

Witt, C. C., Ono, Y., Puschmann, E., McNabb, M., Wu, Y., Gotthardt, M., Witt, S. H., Haak, M., Labeit, D., Gregorio, C. C. et al. (2004). Induction and myofibrillar targeting of CARP, and suppression of the Nkx2.5 pathway in the *mdm* mouse with impaired titin-based signaling. *J. Mol. Biol.* **336**, 145-154. doi:10.1016/j.jmb.2003.12.021